Available online at www.sciencedirect.com
SCIENCE DIRECT
Composites: Part A 37 (2006) 438–446
composites
Part A: applied science and manufacturing
www.elsevier.com/locate/compositesa

Effect of soy protein concentrate in elastomer composites

L. Jong[1,*]

United States Department of Agriculture, National Center for Agricultural Utilization Research, Agricultural Research Service, 1815 North University Street, Peoria, IL 61604, USA

Received 2 December 2004; revised 10 May 2005; accepted 16 May 2005

Abstract

Soy protein concentrate (SPC) is an abundant renewable material and is more economically favorable than soy protein isolate. SPC contains both soy protein and soy carbohydrate. An aqueous dispersion of SPC was blended with styrene-butadiene latex to form elastomer composites. The inclusion of soy carbohydrate in addition to soy protein in the composites increased the shear elastic modulus in the small strain region as well as improved the recovery behavior in the non-linear region. At small strain, the equilibrium elastic modulus of 30% filled composites at 140 °C was about 600 times higher than that of the unfilled elastomer, indicating a significant reinforcement effect generated by SPC. Compared with soy protein isolate, the stress softening effect and recovery behavior under dynamic strain indicated that the addition of soy carbohydrate might have increased the filler–rubber interaction. The behavior of modulus decrease with increasing strain is also different between SPC and protein composites.
Published by Elsevier Ltd.

Keywords: A. Particle-reinforcement; B. Mechanical properties; B. Rheological properties; Soy protein concentrate

1. Introduction

Soy protein concentrate (SPC) is a soy product after soy whey (soluble carbohydrate) is removed from defatted soy flour. Dry SPC is a rigid material and it contains both soy protein and insoluble soy carbohydrate. A few recent investigations have been made on the modulus enhancement of rubbers by natural materials, for example, oil palm wood [1], crab shell chitin [2], and bamboo fiber [3]. From the perspective of renewable materials and environmental reasons, soy protein and other soybean products have been investigated as a component in plastic and adhesive composites [4–8], but have been rarely investigated as a reinforcement component in elastomers. Dry SPC has a shear elastic modulus of ~3 GPa under ambient conditions. Because the high rigidity of a reinforcement phase is one of the requirements in rubber reinforcement, dry SPC is therefore a possible candidate for this application. Attempts to use protein in rubber latex can be traced back to the 1930s. A few patents [9–11] had claimed the use of protein in rubber composites. For example, Lehmann and coworkers [11] had demonstrated the use of casein (milk protein) in natural rubber latex to achieve approximately a fourfold increase in the modulus. Protein as an additive in rubber materials also has been claimed to improve the antiskid resistance of winter tread tires [12–14]. In rubber reinforcement, factors such as aggregate structure, effective filler volume fraction, filler rubber interaction and elastic modulus of filler clusters have important impact on the modulus of rubber composites [15].

Previously, globular soy protein aggregates were used to reinforce styrene-butadiene (SB) rubber and indicated a significant reinforcement effect in the small strain region [16]. However, soy protein isolate is not as economically favorable as soy protein concentrate. Soy protein concentrate contains both soy protein and insoluble soy carbohydrate and is obtained after water-soluble whey (soluble carbohydrate) is removed from defatted soy flour. The objective of this investigation is to compare its reinforcement effect with soy protein isolate to obtain some information on the effect of insoluble soy carbohydrate.

* Tel.: +1 309 681 6240; fax: +1 309 681 6685.
E-mail address: jongl@ncaur.usda.gov.

[1] Names are necessary to factually report on available data; however, the USDA neither guarantees nor warrants the standard of the product, and the use of the name by USDA implies no approval of the product to the exclusion of others that may also be suitable.

1359-835X/$ - see front matter Published by Elsevier Ltd.
doi:10.1016/j.compositesa.2005.05.042

In this study, the rubber matrix chosen was a styrene-butadiene rubber with a small amount of carboxylic acid-containing monomer units, because previous studies have indicated the importance of the interaction between filler and matrix [17]. Soy protein contains a significant amount of carboxylic acid and substituted amine groups [18]. The insoluble soy carbohydrate is also capable of interacting with carboxylic functional groups in the SB matrix through hydrogen bonding and ionic interaction. Structurally, soy protein is a globular protein and its aggregate is similar to colloidal aggregates, but soy carbohydrate is a non-globular and film-forming material. For practical applications, the issue of moisture sensitivity in some applications is always associated with natural materials, but it may be improved through product formulation and/or selective applications. For example, it may be used as a component in multi-layered structures, in coated objects, in elevated temperature applications or as a rubber part in greasy/oily environments where the moisture effect is minimal.

The rubber composites investigated here were prepared by casting films from the dispersion of SPC and carboxylated styrene-butadiene latex. To give some background on the rubber matrix of this composite, the properties of carboxylated SB rubber will be described briefly. Carboxylated SB rubber is classified as an ion-containing polymer where the viscoelastic properties are affected by molecular weight, degree of crosslinking, glass transition temperature (T_g), copolymer composition, the number of ionic functional groups, the size of ionic aggregation, the degree of neutralization, and the size of the neutralizing ions [19,20]. Previous studies also have shown honeycomb-like structures in the film of carboxylated latexes due to higher concentration of carboxylic acid groups on the particle surface [21]. Mechanically, the elastic modulus of base rubber is not significant when compared with the modulus of the filler network in highly filled elastomeric composites [17].

2. Experimental procedures

2.1. Materials

The defatted soy flour (DSF) used in this research was a spray dried powder (Nutrisoy 7B, Archer Daniels Midland Company, Decatur, IL). Sodium hydroxide, used to adjust pH, was ACS grade. Soy protein concentrate (SPC) was obtained by coagulating an 11% DSF dispersion at pH 4.5 followed by centrifuging at 3000 rpm for 10 min. The process was repeated three times and the resulting paste with a solid content of 22% was used to prepare rubber composites. Soy protein used in this research is a slightly enzyme hydrolyzed soy protein isolate (PRO-FAM 781, Archer Daniels Midland Company, Decatur, IL). It contains more than 90% protein, ~6% ash and ~4% fat. The carboxylated styrene-butadiene (SB) latex was a random copolymer of styrene, butadiene, and small amount of carboxylic acid-containing monomers [21] (CP 620NA, Dow Chemical Company, Midland, MI). The glass transition temperature of carboxylated SB Latex is ~10 °C determined by differential scanning calorimetry. Seven carboxylated styrene butadiene latexes (Ameripol Synpol) with T_g ranged from −5 to 17 °C and styrene content ranged from 57 to 67% were used as an empirical calibration curve to estimate the styrene/butadiene ratio. The styrene/butadiene ratio estimated from the T_g was approximately 65/35. The dried latex is not known to be soluble in any solvent or a combination of solvents. The latex received had ~50% solids and a pH ~6. The volume weighted mean particle size of the latex was ~0.18 μm.

2.2. Preparation of elastomer composites

SPC was first dispersed in water and the pH was adjusted to 9 with sodium hydroxide and then mixed with SB latex already adjusted to pH 9. The ratio of ~5 wt% SPC dispersion vs. SB latex was varied to prepare dry composites containing 10–30 wt% of SPC. The composites were prepared by first casting an emulsion of the blend onto an aluminum mold covered with a Teflon release sheet (BYTAC from Saint-Gobain Performance Plastics) and then allowing them to dry at 75 °C for 72 h. After drying, the samples were removed from the mold and annealed at 110 and 140 °C for 24 h, respectively. The film of 100% carboxylated SB rubber was prepared by adjusting the pH of latex to 9 and drying under the same conditions as that of the SPC/SB composites. The soy protein composites (Soy/SB) were also prepared by the same procedure. The dried carboxylated SB film contained less than 0.3% moisture and the dried SPC/SB and Soy/SB composites had moisture contents less than 0.8% as measured by a halogen moisture analyzer (Mettler Toledo HR73) at 105 °C for 60 min. For the 100% SPC and soy protein, torsion bars could not be made by the casting method. The freeze-dried powder was compression molded at 44 MPa and 140 °C for 2 h. After compression molding, the samples were relaxed at 140 °C for 24 h. The weight fractions of soy protein in the composites were converted to volume fractions by measuring the density of SPC, soy protein, and SB. In these density measurements, a low viscosity poly(dimethyl-siloxane) was used as an immersion liquid and the component volumes were assumed to be additive.

2.3. Scanning electron microscopy

The morphology of SPC and soy protein aggregates was examined by scanning electron microscopy (SEM) using a JEOL JSM-6400V instrument. Images of these soy products were obtained by casting onto an aluminum substrate a dilute dispersion of SPC or protein at pH 9 and at a concentration of 0.004%. The samples on aluminum stubs

were then coated with Au–Pd and examined under vacuum at ambient temperature.

2.4. Particle size measurements

The mean particle size and distribution of SPC and protein aggregates were measured by using a Horiba LA-930 laser scattering particle size analyzer with the red light wavelength of 632.8 nm and the blue light wavelength of 405 nm. The measurement is based on Mie scattering theory and has a measurement range of 0.02–2000 μm. The volume weighted mean diameter of 0.17 μm was obtained for the styrene-butadiene latex and was in good agreement with the particle size value of 0.18 μm supplied by Dow Chemical Company.

2.5. Dynamic mechanical measurements

A Rheometric ARES-LSM rheometer was used in all dynamic mechanical measurements. Temperature ramp experiments (Fig. 1) were conducted using a torsional rectangular geometry with a heating rate of 1 °C/min and a temperature range from −40 to 140 °C. The soak time at each temperature after ramp was 15 s and the measurement duration at each temperature was 30 s. When using torsion rectangular geometry, torsional bars with dimensions of approximately 40×12.5×3 mm were mounted in the torsion rectangular fixtures and the dynamic mechanical measurements were conducted at a frequency of 0.16 Hz (1 rad/s) and a strain of 0.05%.

For all strain sweep experiments, the oscillatory storage and loss moduli, $G'(\omega)$ and $G''(\omega)$, were measured using a torsional rectangular geometry. A rectangular sample with dimension of approximately 12.5×20×3 mm was inserted between the top and bottom grips. The gap between the fixtures was 5–6 mm in order to achieve a strain of ∼15%. A sample length shorter than 5 mm is not desirable because of the shape change from the clamping at both ends of the sample. The frequency used in the measurements was 1 Hz. The oscillatory storage and loss moduli were measured over a strain range of approximately 0.007–15%. The actual strain sweep range was limited by sample geometry and motor compliance at large strain, and by transducer sensitivity at small strain. Although harmonics in the displacement signal may be expected in non-linear material, a previous study [22] indicated that the harmonics are not significant if the shearing strain does not exceed 100%. Each sample was conditioned at 80 or 140 °C for 30 min and then subjected to eight cycles of dynamic strain sweep in order to study the stress softening effect.

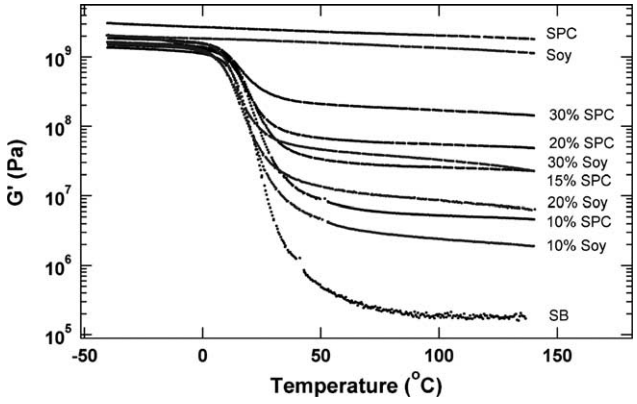

Fig. 1. Storage moduli of SPC/SB and Soy/SB composites. The weight fraction of filler is indicated at the end of each curve.

3. Results and discussions

3.1. Shear elastic modulus

As shown in Fig. 1, the addition of SPC dispersion into styrene-butadiene rubber caused a significant reinforcement effect in the rubber plateau region. The reinforcement effect was proportional to the SPC content. Comparing SPC and soy protein filled composites at 20 and 30% concentrations, the difference in the moduli was significant between these two composites. The elastic moduli of 100% SPC and soy protein are also shown in the top portion of Fig. 1. SPC prepared under the same condition as that of soy protein exhibited a higher elastic modulus. The higher rigidity of

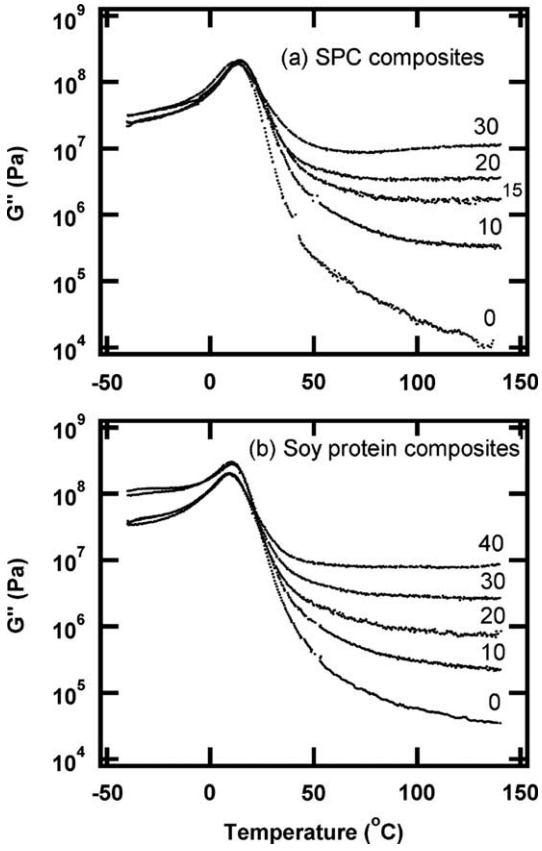

Fig. 2. (a) Loss modulus (G'') of SPC composites. (b) Loss modulus (G'') of soy protein composites.

SPC accounts for part of the reason that the elastic moduli of its composites were higher than that of soy protein in the small strain region. Other factors include the difference in filler–rubber interaction in the stress softening effect that will be discussed later. The glass transition temperatures are, however, not affected by the inclusion of these fillers due to their larger aggregate size and limited surface area. The T_g of SPC and soy potein composites did not show any significant shifting as the filler concentration was increased from 0 to 40% (Fig. 2). The broadening of G'' transition as the filler content is increased may indicate the effect of filler immobilized polymer phase. A better understanding can be made by examining the SEM pictures of both SPC and soy protein in Fig. 3. Fig. 3(a) shows that soy protein aggregates are embedded in the film-like soy carbohydrate. Comparing with Fig. 3(b), it is clear that soy protein aggregates have globular structure, while soy carbohydrate has a film-like structure. To examine whether soy carbohydrate can behave as an adhesive network to bridge the soy protein aggregates, the aggregate size measurements were conducted in water under ultrasonic dispersion. The size distribution curves are shown in Fig. 4. After both SPC and soy protein dispersion were subjected to the same ultrasonic dispersion for the same period, soy protein aggregates were significantly reduced in size while the SPC only changed slightly.

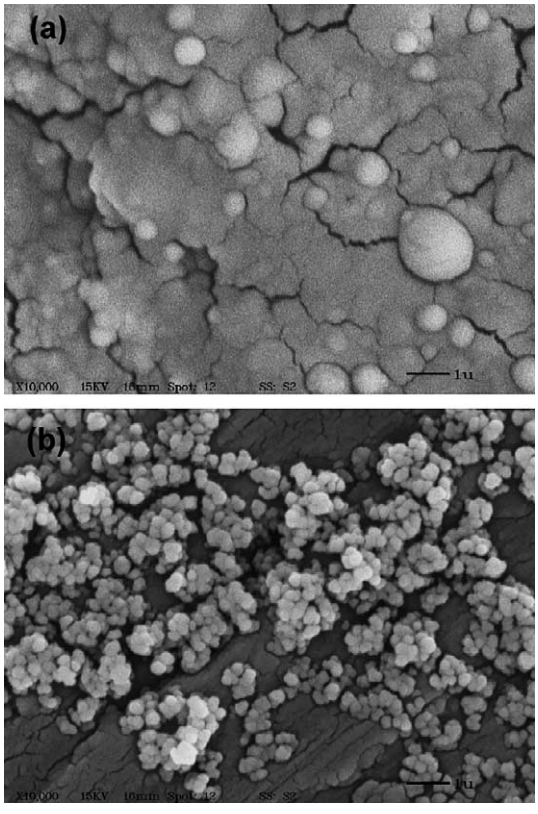

Fig. 3. (a) The SPC film on an aluminum substrate showing the soy protein aggregates are embedded in the soy carbohydrate film. (b) Soy protein aggregates on a gray mottled aluminum substrate. The scale of black bar located at the right bottom corner is 1 μm.

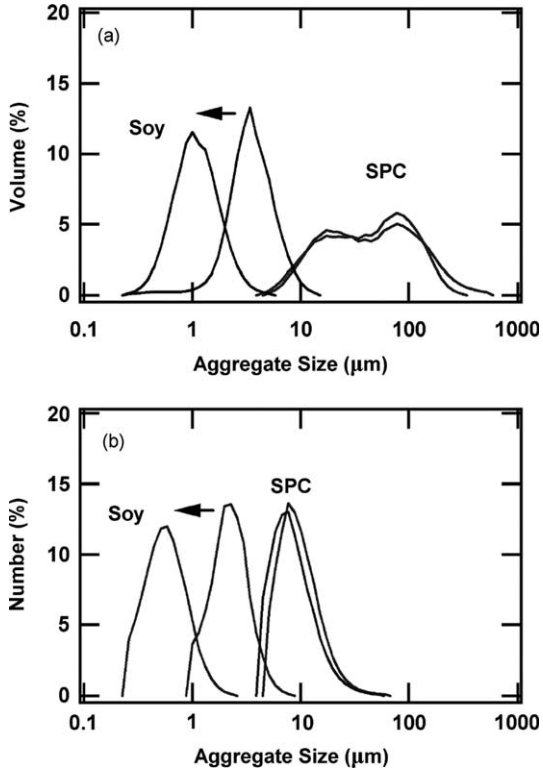

Fig. 4. The measurements of volume weighted aggregate size in water. Both SPC and soy protein aggregates were subjected to one hour of ultrasonic dispersion. Aggregate size of soy protein could be significantly reduced and the size distribution curve was shifted to the left, while that of the SPC only changed slightly.

This indicates the protein embedded SPC aggregates are strong and the soy carbohydrate is capable of holding the protein aggregates together. This effect is also expected to be operating in the composites in terms of enhancing the filler network strength in the small strain region. The significant difference between the volume and number distribution of SPC dispersion in Fig. 4 indicates a substantial inhomogeneity in the SPC dispersion. Based on volume average size in water, SPC has a mean diameter of ~66 μm and a size range of 5–500 μm. Soy protein aggregates has a mean diameter of ~4 μm and a size range of 1–15 μm.

Another difference between SPC and soy protein composites is that the elastic moduli of soy protein composites decreased more rapidly with increasing temperature, whereas the elastic modulus of SPC composites tended to decrease slowly with temperature and then reached a plateau value. This was most evident in the temperature range above ~75 °C as shown in Fig. 1. This is an interesting indication that the strength of filler network structures of these two types of fillers in the composites is different. This also indicates the SPC filled rubber composites have better high temperature stability, whereas the network structure of soy protein aggregates are weakened by the increasing temperature.

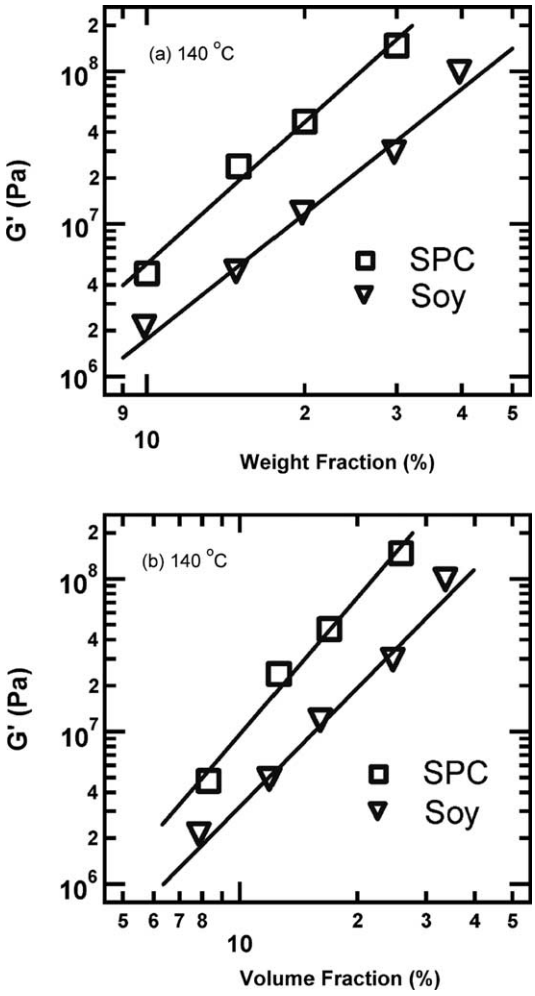

Fig. 5. Elastic moduli of SPC and Soy composites in the small strain region plotted against weight and volume fractions. The measurements were conducted at 0.16 Hz and 140 °C.

In the rubber plateau region, the elastic moduli of SPC and soy protein composites were plotted against the weight and volume fraction of fillers (Fig. 5). The SPC generated a more significant reinforcement effect than the soy protein in the concentration range studied, and the difference between the moduli of SPC and that of the soy protein was greater in the higher concentration region than the lower concentration region. From the slope of elastic modulus vs. volume fraction, it was observed that the modulus of SPC composites increased more rapidly than that of the protein composites. The slope of plots in Fig. 5(b) is ~3 for SPC composites and is ~2.6 for soy protein composites. Overall, SPC showed a substantial improvement over protein in the reinforcement of elastomer.

3.2. Stress softening effect

The stress softening effect occurs in most filled elastomers. In these systems, the stress required to deform the filled rubber at a given elongation is reduced during the second cycle of deformation. The effect is also called Mullin effect because of his extensive studies on this phenomenon [23,24]. The stress softening effect is generally considered to be caused by filler related structures and therefore can yield some insight into the filler structures [17]. The stress softening effect of 100% styrene-butadiene (SB) rubber, 30% SPC filled styrene-butadiene rubber composite (30/70 SPC/SB), and 30% soy protein filled styrene-butadiene rubber composite (30/70 Soy/SB) is shown in Fig. 6. Similar to carbon black or silica filled elastomers [17], the SPC and soy protein composites show a significant reduction in the shear elastic modulus after the first strain cycle. At 80 °C, the strain sweep curves for both 30/70 SPC/SB and Soy/SB composites become more reproducible after four cycles of dynamic strain. 100% styrene-butadiene rubber also shows a stress softening effect, but its contribution to the stress softening effect of the composites is not significant. This is evident by comparing the differences between the first and the eighth strain cycle of shear elastic modulus in Fig. 6(a) and (b). G' difference between the first and the eighth cycle at 0.1% strain is 0.14 MPa for SB and is 96 MPa for the 30/70 SPC/SB composite. The contribution of stress softening effect from the rubber is less than 0.5% in the 30/70 SPC/SB or 30/70 Soy/SB composites. The stress softening effect in SPC/rubber composites comes mostly from the contribution of the SPC related structures such as the SPC network and SPC–rubber interactions. The increasing magnitude of strain (deformation) in the first four strain cycles apparently causes the filler network to break down and possibly the polymer chains to detach from the filler aggregates. In this aspect, the current SPC/rubber composites are not very different from the well-known carbon black filled rubber composites. After four strain cycles, filler related network structures can be broken and reformed and is an indication of reaching an equilibrium condition. The mechanism of agglomeration and de-agglomeration of fillers is based on the elasticity of the filler-immobilized rubber network and not from the elasticity of the filler network, because the rigid filler network is broken when it is deformed beyond the small strain region. The recovery of the deformed composite therefore comes entirely from the elasticity of the filler-immobilized rubber shell around the fillers. The network structure of the immobilized rubber shell around the filler network is a reflection of filler structure and therefore can be characterized by the filler structure. The immobilized rubber network is analogous to a rubber with a higher crosslinking density and therefore has a better memory to return to its original shape when compared to a rubber with a lower crosslinking density. A stronger interaction between the filler and the rubber matrix has been shown to be effective in improving modulus recovery [25].

For loss modulus under cyclic strain, the energy dissipation process became less pronounced and the maxima were shifted to the lower strain amplitudes. The structure responsible for the energy dissipation process is

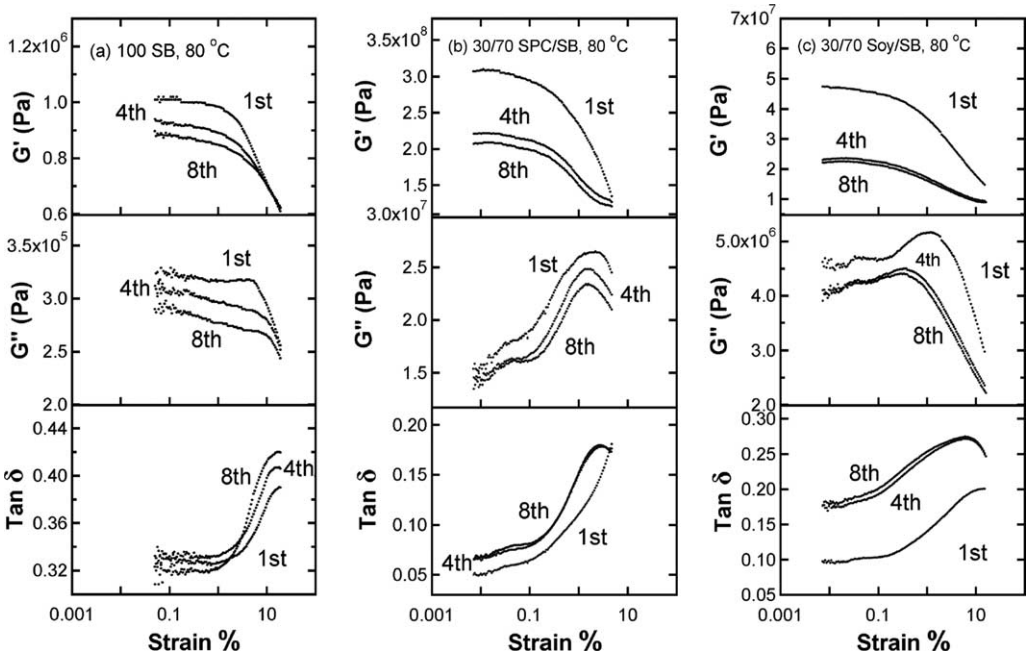

Fig. 6. Elastic modulus (G'), loss modulus (G''), and loss tangent (Tan δ) were measured in the strain sweep experiments: (a) 100% SB at 80 °C (b) 30/70 SPC/SB composite at 80 °C (c) 30/70 Soy/SB composite at 80 °C.

apparently reduced after the first four cycles. In the eighth strain cycle, the value of Tan δ within 0.1–1% strain is 0.08–0.15 for the SPC composite (Fig. 6(b)) and is 0.2–0.25 for the protein composite (Fig. 6(c)). The same trend was also observed in the lower strain region of 0.01–0.1% strain. The lower damping of the SPC composite indicates the SPC composite has a stronger structure than the protein composite.

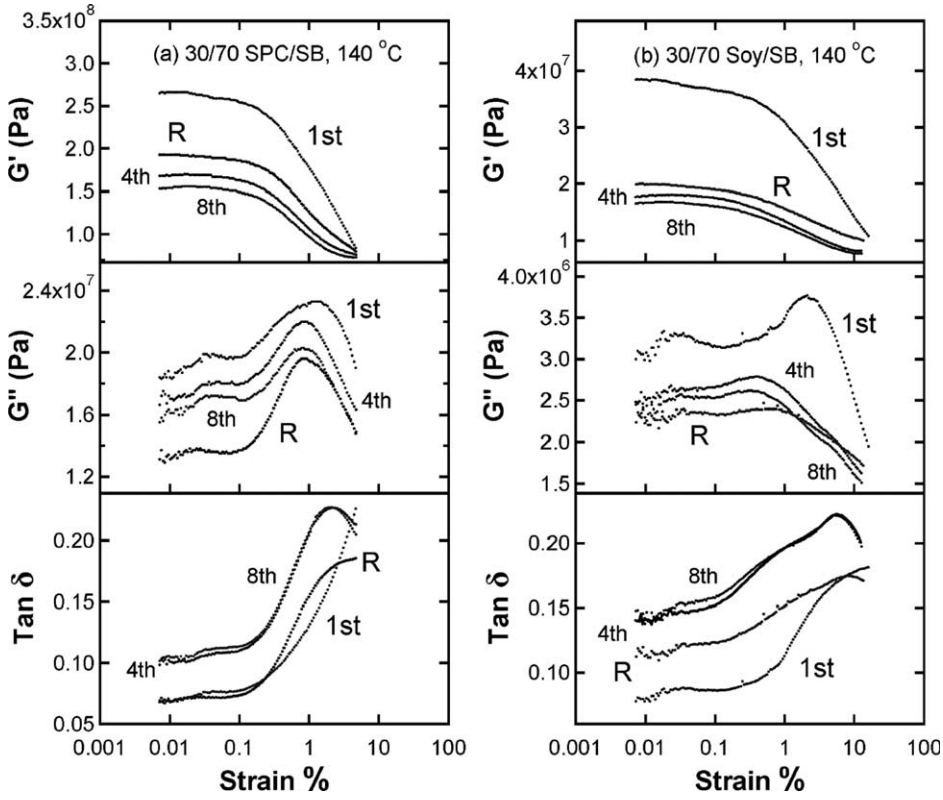

Fig. 7. Elastic modulus (G'), loss modulus (G''), and loss tangent (Tan δ) were measured in the strain sweep experiments: (a) 30/70 SPC/SB composite at 140 °C (b) 30/70 Soy/SB composite at 140 °C. *R* indicates the recovery curve after the samples are conditioned at 140 °C for 24 h.

The magnitudes of shifting in the position of loss maxima in Fig. 6(b) and (c) are also different. At 80 °C, the Soy/SB composite in Fig. 6(c) exhibits a loss maximum at 1.2% strain in the first cycle, whereas SPC/SB composite in Fig. 6(b) has a loss maximum at 2.2% strain in the first cycle. In the eighth cycle, the loss maximum of protein composite occurs at 0.3% strain and that of the SPC composite occurs at 1.5% strain. A greater shifting of loss maximum towards the lower strain at the eighth cycle in the protein composite may indicate the protein related network structure is slower to recover than that of the SPC composite within the same period. This is not an effect of filler volume fraction, since the densities of SPC (1.35 g/cm^3) and soy protein (1.3 g/cm^3) are similar. At 140 °C, the same phenomenon was again observed in Fig. 7. This observation is also consistent with the recovery curves shown in Fig. 7(a) and (b), where the SPC composite recovered 73% of its G_0' and the soy protein composite only recovered 52% of its G_0'. The percentage of recovery is defined here as the fraction of its initial elastic modulus at 0.01% strain (first cycle), but not the recovery from the modulus at the eighth cycle. This indicates that the SPC composite had a better recovery in the modulus values than that of the protein composite under the same conditions. Previously, it was shown that a stronger filler–rubber interaction could yield a better recovery behavior [25]. Therefore, a stronger SPC–rubber interaction in the SPC composites compared with that of the soy protein can explain these recovery behaviors.

3.3. Elasticity of SPC related rubber structures

In order to obtain more information on the reinforcement effect of SPC, the composites were subjected to oscillatory strain at different magnitudes similar to the previous stress softening experiments. The shear elastic moduli of filled elastomers with 20 and 30% of SPC and soy protein aggregates are shown in Fig. 8. The data shown is the eighth cycle of strain sweep. The resulting modulus–strain spectra are similar to that of carbon black [17]. The reduction of shear elastic modulus with increasing strain is a familiar phenomenon reported by Payne on carbon black filled rubbers in the early 1960s. Later Kraus [26] proposed a phenomenological model based on Payne's idea of filler networking. The model is based on the aggregation and de-aggregation of carbon black agglomerates. In this model, the carbon black contacts are continuously broken and reformed under a periodic sinusoidal strain. Based on this kinetic aggregate forming and breaking mechanism at equilibrium, elastic modulus was expressed as follows:

$$\frac{G'(\gamma) - G'_\infty}{G'_0 - G'_\infty} = \frac{1}{1 + (\gamma/\gamma_c)^{2m}} \quad (1)$$

where G'_∞ is equal to $G'(\gamma)$ at very large strain, G'_0 is equal to $G'(\gamma)$ at very small strain, γ_c is a characteristic strain where $G'_0 - G'_\infty$ is reduced to half of its zero-strain value,

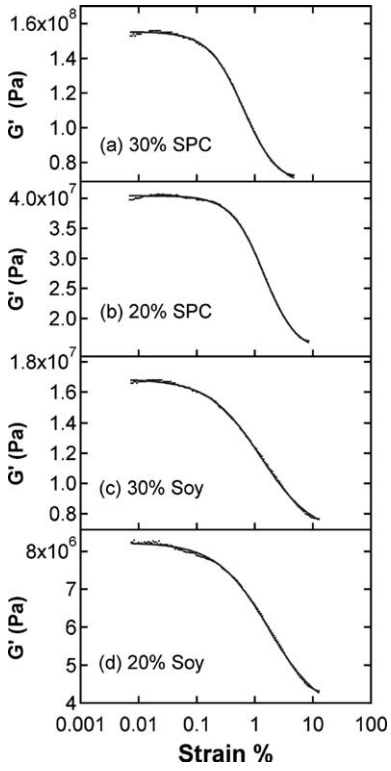

Fig. 8. Elastic moduli of the eighth cycle of strain sweep experiments at 140 °C and 1 Hz. (a) 30/70 SPC/SB composite (b) 20/80 SPC/SB composite (c) 30/70 Soy/SB composite (d) 20/80 Soy/SB composite. Solid lines are the fit from the Kraus model.

and m is a fitting parameter related to filler aggregate structures. Eq. (1) has been shown to describe the behavior of $G'(\gamma)$ in carbon black filled rubber reasonably [15]. The loss modulus and loss tangent, however, do not have a good agreement with experiments [27], mainly due to the uncertainty in the formulation of a loss mechanism. Recently, Huber et al. also modeled the Payne effect and gave a similar expression as the Kraus model, but with a physical interpretation of the fitting parameter m in the Kraus model. Based on the cluster–cluster aggregation (CCA) model, Huber et al. [28] obtained $m = 1/(C - d_f + 2)$, where C is a connectivity exponent related to the minimum path along the cluster structure and d_f is the fractal dimension of clusters. Therefore, the fitting parameter m has a physical meaning related to filler structures or filler immobilized rubber structures. The fractal dimension of fractal-like protein clusters can be estimated from the slope in Fig. 5 by using the strong link model [29] because the protein aggregates form a network above the percolation threshold. The strong link model indicates $\log G'_0 \sim (3 + C)/(3 - d_f) \log \phi$, where ϕ is the volume fraction of particles and C and d_f have been defined previously. C takes a value from 1 to d_f [29]. For soy protein aggregates, d_f is estimated to be 1.35–1.48. The parameter m can be estimated from the fractal dimension of soy protein aggregates and is approximately in the range 0.47–0.65. The agreement between the estimation and the best fit of experimental

Table 1
Fit parameters of shear elastic modulus[a]

Composition	Best fit[b]				
	m		γ_c(%)	G_0'(MPa)	G_∞'(MPa)
SPC/SB	Fourth cycle	Eighth cycle	Eighth cycle	Eighth cycle	Eighth cycle
20/80	0.77±0.02	0.78±0.02	1.42±0.03	40.4±0.1	14.5±0.3
30/70	0.71±0.01	0.73±0.02	0.63±0.02	155.3±0.4	67.2±1.1
Soy/SB					
20/80	0.51±0.02	0.46±0.02	1.88±0.13	8.25±0.03	3.53±0.13
30/70	0.51±0.02	0.46±0.02	1.39±0.07	16.9±0.06	6.20±0.2

[a] Measured at 140 °C.
[b] Best fit of shear elastic modulus vs. strain with the Kraus Model.

data shown in Fig. 8 and Table 1 is reasonable and is similar to that of carbon black composites, $m=0.5-0.6$ [15,30]. For SPC composites, the estimated fractal dimension from Fig. 4 is 1.49–1.65 and the parameter m is estimated to be 0.46–0.74. The estimated range for parameter m is somewhat large due to the uncertainty in the parameter C. Furthermore, the SPC structure consisting of soy carbohydrate embedded with protein aggregates may no longer fit the definition of particle aggregate. Therefore, it may not be appropriate to use fractal-like description for the SPC composites. However, an empirical fit is provided to demonstrate the difference in the curve shapes (Fig. 8) between the SPC and protein composites. In general, the fitting parameter $m\approx0.75$ for SPC composites is obviously different from that of soy protein composites and reflects a difference in their structures shown in Fig. 3.

4. Conclusion

SPC was incorporated at different levels into carboxylated SB elastomers. In the rubber plateau region, a very significant increase in the equilibrium storage modulus of dry composites was observed when compared with that of the 100% carboxylated SB elastomer. The observed significant reinforcement effect was studied by dynamic temperature sweep experiments and compared with that of soy protein. At the same weight fraction of fillers, SPC exhibited a higher reinforcement effect than that of soy protein in the rubber plateau region and had better high temperature stability. The composites were also studied by using the dynamic strain sweep experiments to understand the filler related structures. Both SPC and soy protein structures exhibited similar behavior in terms of reversible structure breakdown after four cycles of dynamic shear strain. The SPC composites exhibited a better recovery behavior after eight cycles of dynamic strain, indicating a stronger filler–rubber interaction. The Payne effect of SPC and protein composites at 140 °C was interpreted using the Kraus model. The fitting parameter m for SPC composites was found to be different from that of soy protein composites. This study indicates that the use of SPC in rubber composites is a better option than soy protein in terms of both composite properties and cost.

Acknowledgements

The author thanks Dr A.R. Thompson for scanning electron microscopy and A.J. Thomas for help with the rheological instruments.

References

[1] Ismail H, Jaffri RM, Rozman HD. The effect of filler loading and vulcanization system on properties of oil palm wood four-natural rubber composites. J Elastomers Plast 2003;35(2):181–92.
[2] Nair KG, Dufresne A. Crab shell chitin whisker reinforced natural rubber nanocomposites. 2. Mechanical behavior. Biomacromolecules 2003;4:666–74.
[3] Ismail H, Shuhelmy S, Edyham MR. The effect of a silane coupling agent on curing characteristics and mechanical properties of bamboo fiber filled natural rubber composites. Eur Polym J 2001;38(1):39–47.
[4] Wang C, Carriere CJ. Blends of biodegradable poly(hydroxy ester ether) thermoplastic with renewable proteins. US Patent 6 310 136 B1; 2001.
[5] Wang S, Sue HJ, Jane J. Effects of polyhydric alcohols on the mechanical properties of soy protein plastics. J M S-Pure Appl Chem 1996;A33(5):557–69.
[6] Paetau L, Chen C, Jane J. Biodegradable plastic made from soybean products. 1. Effect of preparation and processing on mechanical properties and water absorption. Ind Eng Chem Res 1994;33:1821–7.
[7] Mo X, Sun XS, Wang Y. Effects of molding temperature and pressure on properties of soy protein polymers. J Appl Polym Sci 1999;73:2595–602.
[8] Wu Q, Zhand L. Properties and structure of soy protein isolate-ethylene glycol sheets obtained by compression molding. Ind Eng Chem Res 2001;40:1879–83.
[9] Coughlin ETA. Floor covering. US Patent 2 056 958; 1936.
[10] Isaacs MR. Composition of matter. US Patent 2 127 298; 1938.
[11] Lehmann RL, Petusseau BJ, Pinazzi CP. Preparation of rubber–protein–glyoxal composition and vulcanizable material obtained therefrom. US Patent 2 931 845; 1960.
[12] Fuetterer CT. Anti-skid tire treads and rubber stock therefor. US Patent 3 113 605; 1963.
[13] Beckmann O, Teves R, Loreth W. Rubber compounds for treads for winter tires. Ger Offen DE 19622169 A1 19961212; 1996.
[14] Recker C. With sulfur vulcanizable rubber compositions containing proteins from oilseeds for winter tire treads. Eur Pat Appl EP 1234852 A1 20020828; 2002.

[15] Heinrich G, Kluppel M. Recent advances in the theory of filler networking in elastomers. Adv Polym Sci 2002;160:1–44.
[16] Jong L. Characterization of soy protein/styrene-butadiene rubber composites. Compos Part A 2005;36:675–82.
[17] Wang MJ. Effect of polymer–filler and filler–filler interactions on dynamic properties of filled vulcanizates. Rubber Chem Technol 1998;71:520–89.
[18] Garcia MC, Torre M, Marina ML, Laborda F. Composition and characterization of soybean and related products. Crit Rev Food Sci Nutr 1997;37(4):361–91.
[19] Richard J. Dynamic micromechanical properties of styrene-butadiene copolymer latex films. Polymer 1992;33(3):562–71.
[20] Zosel A, Ley G. Influence of cross-linking on structure, mechanical properties, and strength of latex films. Macromolecules 1993;26:2222–7.
[21] Kan CS, Blackson JH. Effect of ionomeric behavior on the viscoselastic properties and morphology of carboxylated latex films. Macromolecules 1996;29:6853–64.
[22] Chazeau L, Brown JD, Yanyo LC, Sternstein SS. Modulus recovery kinetics and other insights into the Payne effect for filled elastomers. Polym Compos 2000;21(2):202–22.
[23] Mullins L. Effect of stretching on the properties of rubber. J Rubber Res 1947;16:275–89.
[24] Mullins L. Thixotropic behavior of carbon black in rubber. Phys Colloid Chem 1950;54:239–51.
[25] Zhu A, Sternstein SS. Nonlinear viscoelasticity of nanofilled polymers: interfaces, chain statistics and properties recovery kinetics. Compos Sci Technol 2003;63:1113–26.
[26] Kraus G. Mechanical losses in carbon-black-filled rubbers. J Appl Polym Sci, Appl Polym Symp 1984;39:75–92.
[27] Ulmer JD. Strain dependence of dynamic mechanical properties of carbon black-filled rubber compounds. Rubber Chem Technol 1995; 69:15–47.
[28] Huber G, Vilgis TA. Universal properties of filled rubbers: mechanisms for reinforcement on different length scales. Kautsch Gummi Kunstst 1999;52:102–7.
[29] Shih W, Shih WY, Kim S, Liu J, Aksay IA. Scaling behavior of the elastic properties of colloidal gels. Phys Rev A 1990;42:4772–9.
[30] Heinrich G, Vilgis TA. Effect of filler networking on the dynamic mechanical properties of crosslinked poymer solids. Macromol Chem Phys, Macromol Symp 1995;93:253–60.